A detailed study on Lift Augmentation conventional techniques used in airfoil

JV muruga lal Jeyan [1*] sumit rade [2] chirag Khanna [3] Suptajyoti Chirui [4]

1* Research supervisor Department of aerospace Lovely professional university

2,3,4 UG scholar Department of aerospace Lovely professional university

Abstract

Purpose – Lift augmentation in aircraft wings has been a major concern since the early age of fixed wing aircrafts. Though a lot of research work has been done on this topic previously there has not been any prominent technique that has outshined all the other techniques in terms of resultant lift augmentation. Thus here is a detailed comparative study about some of the better performing lift augmentation techniques that has used flow separation using various techniques.
Design/methodology/approach – This paper explores the implications of various types of techniques used for flow separation over a naca 4 series aerofoil using different methods.
Findings – Lift augmentation in an airfoil is the process by which we do the flow separation over the top surface of an airfoil through the cross section. There have been several techniques used for this but the most effective flow inject techniques are use of dual vents and piezoelectric oscillating ducts for NACA4 series and other large size aircrafts but these techniques require a great deal of power thus they are not that cost effective in case of small aircrafts.
Practical implications – This paper will help the manufacturers a detailed view with all the different techniques used for flow separation over an airfoil for lift augmentation and will take through the different aspects of their working. This will also show the advantages and disadvantages of all the flow separation techniques. Before the selection of the flow separation techniques one should look into the following aspects :1)Selection of suitable sample airfoil and study of flow separation.2)Comparative study of existing and flow injections design3) Practical implementation of flow injection technique in sample designs.
Keywords - Flow Separation, Lift Augmentation, Flow Injection, Augmentation Techniques for NACA 4 series
Paper type General review

Low-Reynolds-Number Separation on an Aerofoil

LOW-REYNOLDS-NUMBER aerodynamics is important for both military and civilian applications. These requests include a propeller, remote control vehicles, water aircraft, best passenger / passenger aircraft, advanced control devices, high-end cars, and wind turbines. As the size of the natural shrinkage is usually only important near the tip of the foil, flow about two shortcuts have been the focus of more research on low-Reynolds-number aerodynamics

The Reynolds low-key separation bubble can extend across 15% of air space. Accurate prediction of its existence and size is therefore required in the construction of a low-efficiency high-speed system airplane. A typical model of the timing of a laminar separation gun, recorded by Horton, is shown in Figure. The distinguishing features of this laminar separation bubble are

vertical pressure regions similar to the river below the point of separation and the sudden increase in pressure near the reconnection point.Flow views and hot lessons for Brendel and Mueller and LeBlanc show consistent flow within a dead spiritual region beyond the point of separation. In this region, the shear layer rises slightly above the surface. Without change

show that the recurring flow is weak and a layer of shear it is also attached to the lower rivers. The unstable circuit of the separation bar is often described as chaos.

When the Reynolds area number based on the size of the boundary layer is high enough, the natural mutation of the bounded boundary layer results in the expansion of Tollmien-Schlichting(viscous-type) instability. However, there is a low Reynolds number

kingdom (Re <5 x 10^5), this viscous type change will occur only when boundary restrictions are applied. If you are a boundary layer Separately, Kelvin-Helmholtz (inviscid-type) will grow as a result of the inflectional velocity profile. Since Kelvin-Helmholtz's instability causes the shear layer to collapse, which it can be expected that instability is the bubble of separation it will be dominated by large-scale vortex shedding and not small turbulence.

Reynolds no.	Angle of attack, deg	SP	RP	BL	SP_{MWM}	RP_{MWM}	BL_{MWM}
6×10^4	4	0.345	0.957	0.612	NR	NR	NR
1×10^5	4	0.355	0.762	0.407	0.35	0.73	0.38
2×10^5	4	0.407	0.662	0.255	0.40	0.62	0.22
1×10^5	0	0.452	0.885	0.433	0.45	0.87	0.42
1×10^5	7	0.288	0.635	0.347	0.32	0.56	0.24

The main features of the main non-compliant layer were studied by Eppler 387 aerofoil on most sides of the attack and Reynolds numbers. In all study cases, the separation of laminar players on the surface of the aerofoil resulted in a temporary vortex scattering and pairing following downstream. Vortex depletion caused by the ruling wave of instability caused by inflection velocity profile below the separation point. Time-consuming non-compliant computer configuration resulted in a splitting bubble that was significantly similar to a normal mineral.

separation bubble. Mid-term results of the calculation indicates the pressure region of the same area

followed by a sudden increase in divine pressure.

Oscillatory Blowing: A Tool to Delay Boundary-Layer Separation

To prevent division and superior generation the lift is an important element of boundary control.

Traditionally, segregation was delayed by appropriate geometry. The design and flexibility can be spaced either through open spaces. There is growing evidence that the introduction of periodic disturbances across the boundary layer and it can delay fragmentation, no matter how high the flow disturbance.External acoustic excitement is delayed the stability of the stable in the aerofoil s, thereby increasing the maximum height produced by them. Since the most active waves of anger are related to the frequency of the tunnel resonance noise, the effectiveness of this type of entertainment is questionable. In addition, sound pressure levels are approx 150 dB (measured in surface air surface3) required to delay the table by 3-4 deg of incidence was extremely high. Another elevation increase was observed when the level of parasite disturbances measured in the boundary layer near on the leading edge was about 40% of freestream. Inside acoustic excitement from a building near on the leading edge of the air carriage works best for delaying stall and evaluating its negative effects, but the size of the elevator created in this way has not been improved at all.

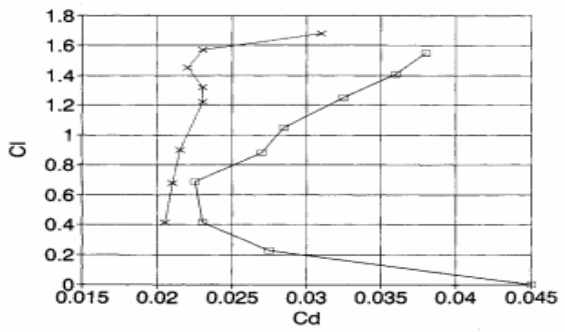

Fig. 2c Vibrating flaperon effect on the drag of an IA1 P255 airfoil.

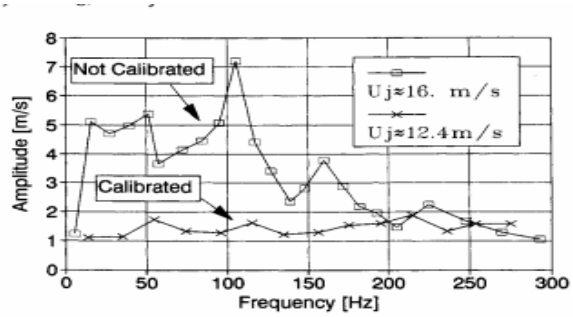

Fig. 3c Oscillatory system frequency response, before and after calibration.

Tests performed on the NACA 0015 air carrier Reynolds numbers from 1 x 10^5 to 1 x 10^6. 365-Mm chord aerofoil fitted with trailing-edge flap for length equal to 25% of its strength (Figure 3a). Wall mural emerged from a two-dimensional structure with a height of H = 1.5 mm. The space is located above the area above the hinge of flap (e.g., at x / c = 0.75). Large internal part the volume of the air that acts as a jet settlement. Pressured air provided a constant source of pressure. The oscillations are provided by a small centrifugal drummer named the inlet and outlet were both connected to the air plenum chamber with a T-type tube junction containing a rotating valve. By placing the valve inside the T-type tube connection, one opens the aerofoil plenum room or exit blower or its input, thus providing oscillatory suction or wind without the flow of net weight. Outstanding frequency of discharge is determined by the rotation level of the valve and its size was determined by pressure provided by the caller and as a result there have been changes in the minute (per minute). Each input was self-controlled and computer-controlled The total jet pressure was divided into two parts: a stable part based on stability beat only and partially oscillatory based on a wide range of variables of velocity. The total pressure value is given by the sum of CM + 0.5, given the maximum velocity perturbation power contained in the frequency of happiness. The whole program was scaled to the file in the absence of external broadcasts of various exit routes and various amplitudes of specified oscillations. The jet speed profile across the specified location was the same as it was the amplitude of the controlled velocity perturbation. Detailed jet measurement measurements are performed in a smart flow of 2H from a pipe where the same jet core and perturbations range it is clearly visible. Exceeding the lift coefficient of the event is constructed (Figure 4a) and polar gravitational pressure (Fig. 4b). Basic Aerofoil features on this flap deviation are also shown in this plan. Fixed explosion at CM = 0.001 is not significant, the effect on raising or dragging the pressure on the sides of events> 4 deg. There are minor errors in Cdp and C / that are associated with the presence of a separation bubble above the flap hinge at this number Reynolds between = - 2 and 4 deg. Convert this fixed beat to (CM) = 0.010 to The reduced frequency based on the flap length is increased and the elevated elevator causes the pressure drop being minimal.

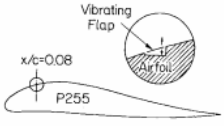

Fig. 2a Vibrating flaperon installation on an IA1 P255 airfoil.

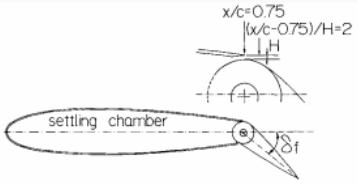

Fig. 3a Flapped and hollow NACA 0015 airfoil.

Delay of Aerofoil Stall by Periodic Excitation

Boundary separation can put a lot of power into its loss and limit functionality of many flow-related functions devices. It imposes severe limitations not only on the design, but the performance of any liquid carrying or moving device. Therefore, control of partition or at least its reduction is always a concern for engineering systems. Geometry construction, tabulators, and synthetic transpiration through Slots and slats are the most commonly used aeronautics for delays separation. Active breathing is scarce. It is very limited in the constant beating of military applications due to

the complexity of the systems and their high power requirements. The Divorce control is being investigated continuously and extensively for its great potential and its many applications, so its state of the art is reviewed from time to time discussed at conferences.

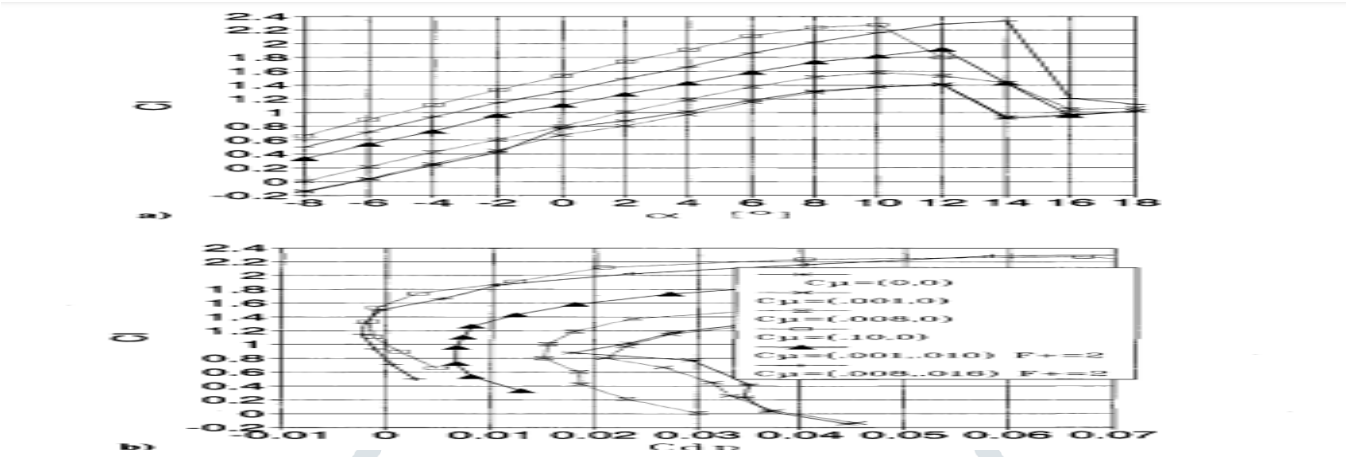

We have long seen that jet penetration can be used to maximize the altitude of airplanes.We also knew that large associated structures can improve internal penetration to move the pressure effectively across the shear layer. We had the idea that a combination of jet and occasional movement could be the most effective tool on border control. This is due to the introduction of time that accelerates and regulates the formation of large concurrent structures, especially when the flow you say is unstable in a given period. As the operation of the method is largely determined by the acceptance of the flow to the standard distraction, this should be at the right level and presented in the right place. Adaptability is provided by setting strong oscillations with minimal solid beats, i.e. may vary according to need. Timeline input contributes to overall momentum and should be calculated with it. Tests were performed on four airplanes on Chord Reynolds numbers ranging from 1.5 X 10^-1 to 1.2 X 10^6 at speed ranging from 6.4 to 51 m / s. The first aerofoil tested was a symmetric NACA 0015 aerofoil with trailing-edge a flap equal to 25% of its weight (Fig. 1). After that all tests performed on integrated airways: 11% Eppler E-214 aircraft with 30% pieces, size 19% PR8-40 aerofoil (manufactured by Israel Aircraft Industries) with 30% smooth flap crush, and 18.3% blunt a plane at the edge with its left slope upward on chord at 45 deg. Oscillatory beats are added in the boundary layer by using small mechanized spaces on the surface of the airplanes. The the location of the actuators is listed in Fig. 1. Most posts are approximately 1 mm and are found above face to knee. One slot was in the lead edge of the NACA 0015 airplane to determine the most appropriate length scale used to reduce the frequency of to attract. The massive blow of the PR8-40 wind came from two different places: one from the edges following the main object while the other from the leading edge of the flap. In this spiritual age we wanted to decide the result of the beating that occurred, which occurred in the middle of the masses element and flap, in area operation from presented by the disruption

The presentation of the two appearances, from time to time the intricate boundary layer enables it to withstand large pressure gradients without splitting. It therefore increases the ascent and reduces the drag caused by aerofoil s to incident angles and flap deviations where flow could not be separated in any other way. In order to effectively control the split, the magnitude of the set oscillations must be increased near the area of ecosystems, and very much so the effective position of the actuator corresponds to this point except that the flow of the ascending boundary layer increases the specified output. The operation of the method is not restricted by the beginning of the first version, the firmness that already exists a confusing border layer, or to change Reynolds' number. This method is very similar to a vertical vortex generator importing smart vortices at a very young age.

CFD ANALYSIS OF CONTROLLING THE AIRFLOW OVER AEROFOIL S USING DIMPLES

Summary:

At present various types of surface alterations are made for delaying the separation of flow, most used is the vortex generator. This study is an attempt to improve the overall aerodynamic properties of an aerofoil by implanting the dimple-shaped surface alterations. We have implanted 12 dimples on both surfaces, upper and lower. Efforts has been made to show that the dimples can also be used to reduce the pressure drag. Dimples are ineffective at 0^{o}AoA but shows a significant decrease in the pressure drag at higher angle of attack. First 2D analysis of inward and outward dimpled NACA-0018 aerofoil was done. The dimples showed a significant increase in the overall aerodynamic performance. Several distinct dimple shapes were studied to find out the best shape and position on the aerofoil surface using the CFX tools in ANSYS. A comparative study was also performed to show the variations of lift and drag of the modified aerofoils at different angle of attack with and without the dimpled surface. A study of turbulent flow over the dimpled aerofoil was performed by using the program ANSYS FLUENT. It showed a significant decrease in the pressure and drag over the surface.

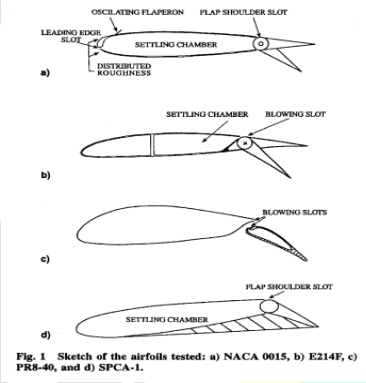

Fig. 1 Sketch of the airfoils tested: a) NACA 0015, b) E214F, c) PR8-40, and d) SPCA-1.

Modelling and Simulation:

A symmetrical NACA-0018 aerofoil with 1m chord and wingspan of 2.5m was used for this study. 12 dimples were put at 18cm from the leading edge on both sides of the wing with similar proportion. The analysis was done at two speeds and four different angles of attack. Modelling was done with the CATIA V5 software and grid creation was done with ICEMCFD software.

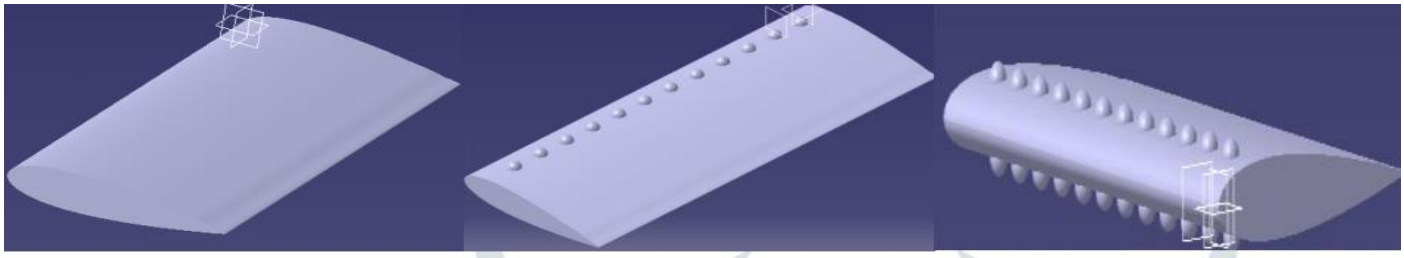

Figure1. Cad model of wing with various dimple configurations

Discussion:

a) Wing Pressure contour at α = 0° and Velocity = 30 m/s

Without dimples upper surface dimples upper and lower surface dimple

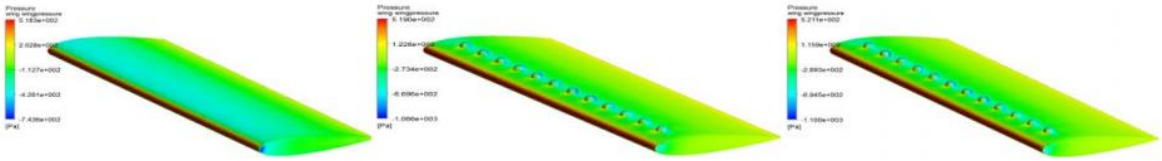

b) Wing Pressure contour at α = 5° and Velocity = 30 m/s

Without dimples upper surface dimples upper and lower surface dimple

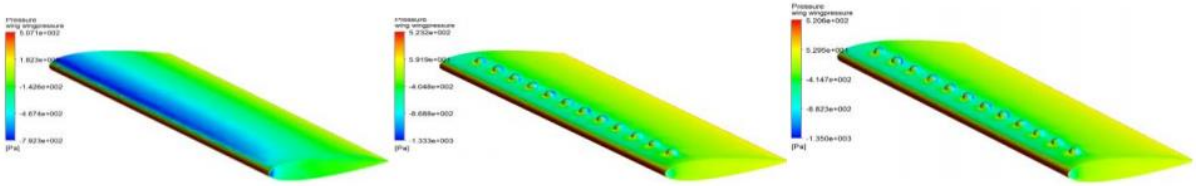

c) Wing Pressure contour at α = 10° and Velocity = 30 m/s

Without dimples upper surface dimples upper and lower surface dimple

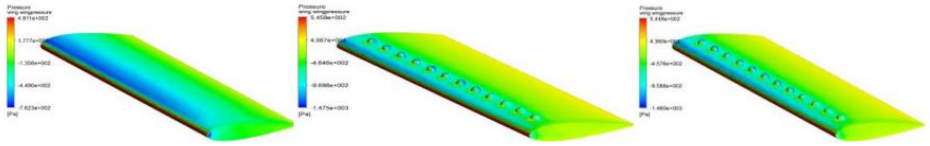

d) Wing Pressure contour at α = 15° and Velocity = 30 m/s

Without dimples upper surface dimples upper and lower surface dimple

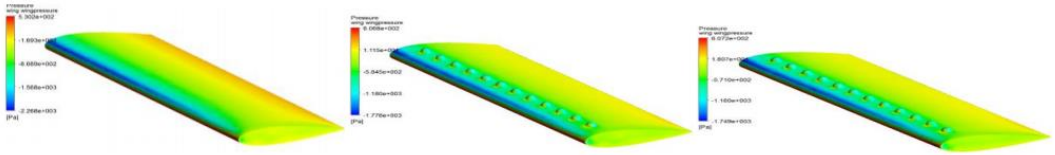

e) Wing Pressure contour at α = 0° and Velocity = 60 m/s

Without dimples upper surface dimples upper and lower surface dimple

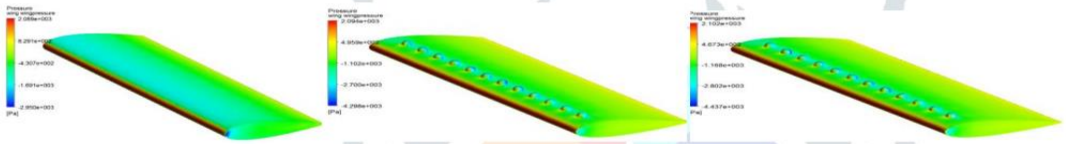

f) Wing Pressure contour at α = 5° and Velocity = 60 m/s

Without dimples upper surface dimples upper and lower surface dimple

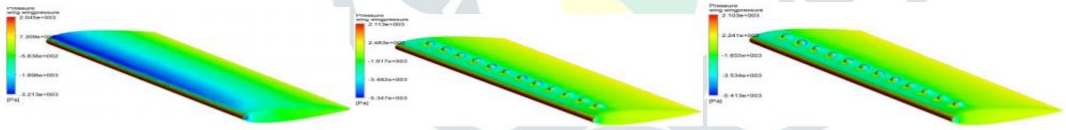

g) Wing Pressure contour at α = 10° and Velocity = 60 m/s

Without dimples upper surface dimples upper and lower surface dimple

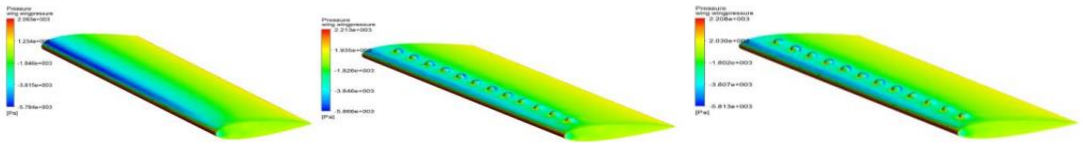

h) Wing Pressure contour at α = 15° and Velocity = 60 m/s

Without dimples upper surface dimples upper and lower surface dimple

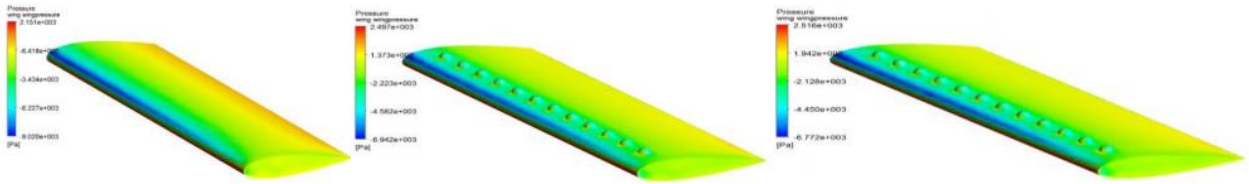

Figure 2: Wing pressure contour for various wing configurations

In figure 2 wing pressure contour is shown for different angle of attack and velocity. From figure 2a to 2d pressure distribution over the wing surface at 30 m/s is shown. The low-pressure region for the dimpled wing profile is less than the smooth one when angle of attack is increased and there was no flow separation as vortices were formed by the dimples. From figure 2e to 2h pressure distribution at 60 m/s is shown. In this slow field also, the low-pressure region was reduced by the introduction of dimples.

Lift Coefficient Curve

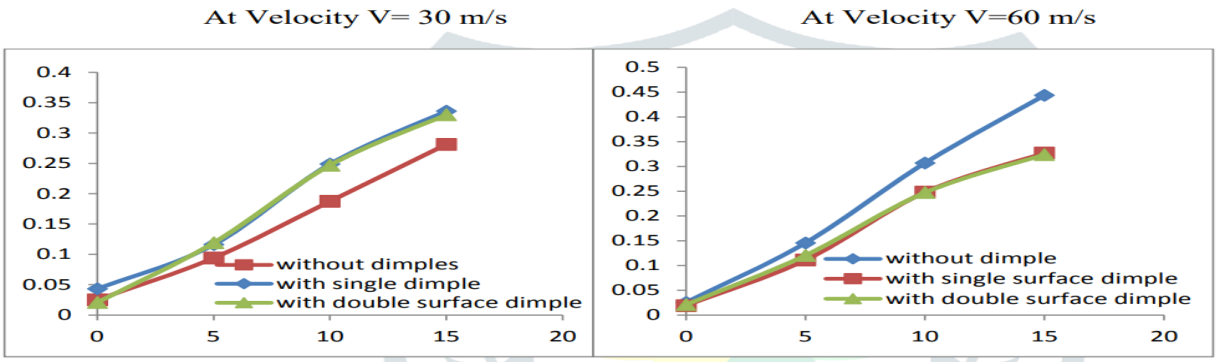

Figure 3: Lift coefficient Vs AOA

Drag Coefficient Curve

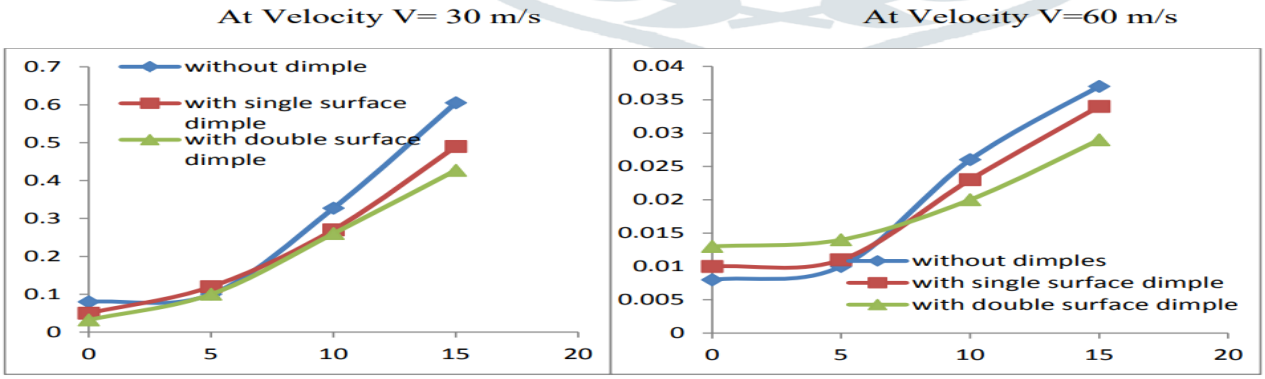

Figure 4: Drag coefficient Vs AOA

In figure 3 the variation of lift coefficient with different AoA at 30 m/s and 60 m/s is shown. At 30 m/s the lift curve for with and without dimpled profile is similar, but at 60 m/s it is lower for the dimpled profile. In figure 4 the variation of drag coefficient with different AoA at 30 m/s and 60 m/s is shown. The dimpled profile showed high drag than the smooth profile.

Aerodynamic Performance Curve

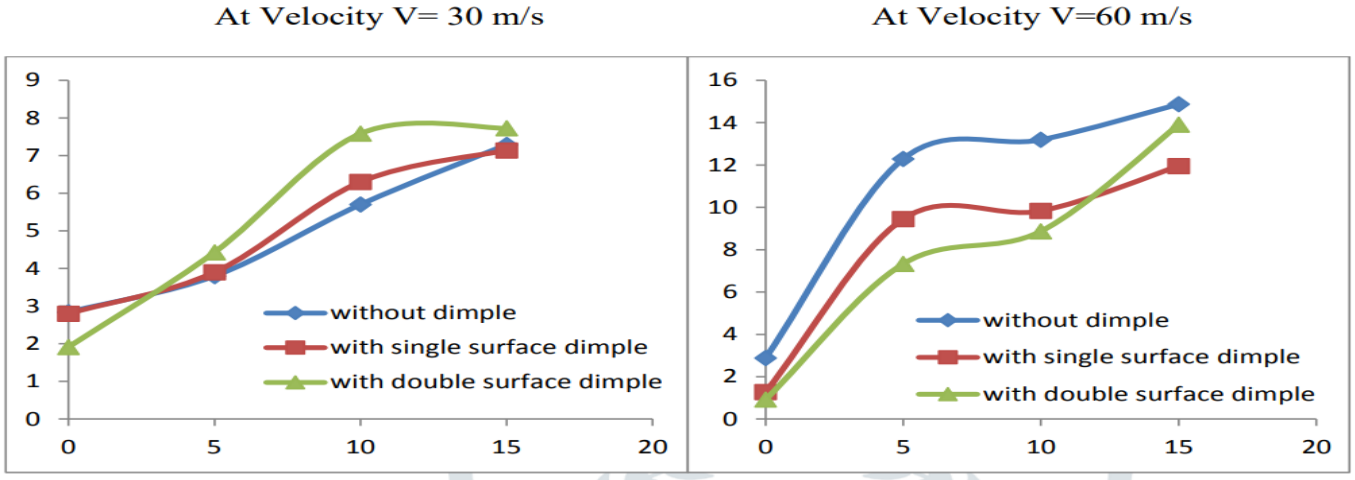

Figure 5: Lift to Drag ratio Vs AOA

In figure 5 variation of L/D with angle of attack is shown. At 30 m/s L/D is maximum for double surface dimple at 10^{o}AoA. At 60 m/s the drag is more for dimpled profile, so L/D is lower than the simple profile.

Conclusion:

Implanting dimples over the surface of the wing is proved to be successful in altering the flow direction. The implementation of the dimples over the surface also improves the overall aerodynamic performance, but it can only be used at low speeds as it is ineffective at higher flow velocities.

Use of Piezoelectric Actuators for Aerofoil Separation Control

Summery: Anaddition of cyclic vortical stress to a boundary layer delays flow separation and eliminates its associated adverse effects in an effective manner.

1 The range of Reynolds numbers at which the experiments were carried out was recently extended to 38X10^6 , demonstrating the validity of the control parameters at right Reynolds numbers.

2 Most of the experiments performed to date have used external laboratory devices to generate the perturbations,and the net efficiency of the system has not been considered.

Presently, surface-mounted piezoelectric actuators are used to excite the turbulent boundary layer upstream of separation, where the actuators interact directly with the boundary layer. The actuators are rigid and do not attenuate with increased aerodynamic loading up to the maximum tested speed of 30m/s.It is demonstrated that these actuators are effective as well as energy efficient.

Procedures:

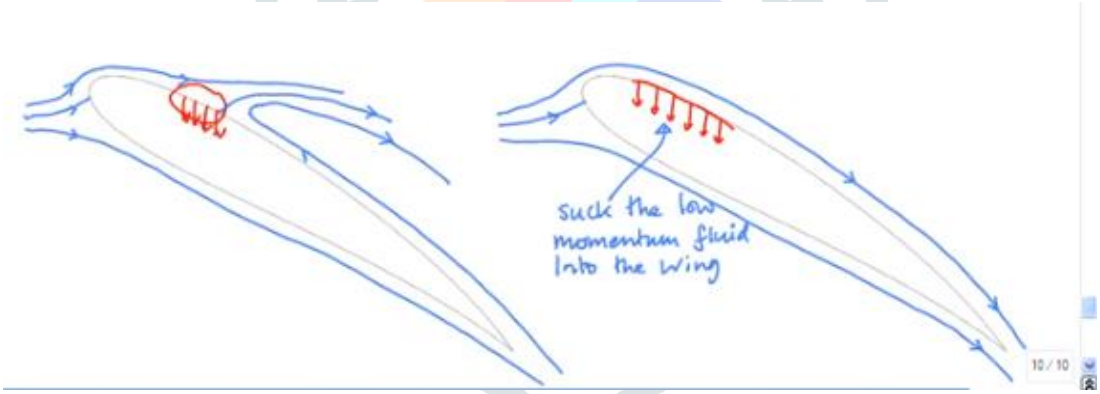

1) 2 Dimensional (All the actuators working identically)
2) 3 Dimensional (Alternative actuators working identically)

Arrangements: A channel 35.5 mm wide, 605 mm long, and 8.5 mm deep was machined in the aerofoil upper surface. Ten actuators were mounted along the span of the aerofoil , flush-mounted to its upper surface, with 0.5-mm gaps between adjacent actuators and between the actuators and the cavity walls. Each actuator was isolated electrically from the aerofoil and connected individually to the driving system to allow full control of the phase and amplitude. The resonance frequency of the actuators was tuned identically to within +-0:5 Hz.

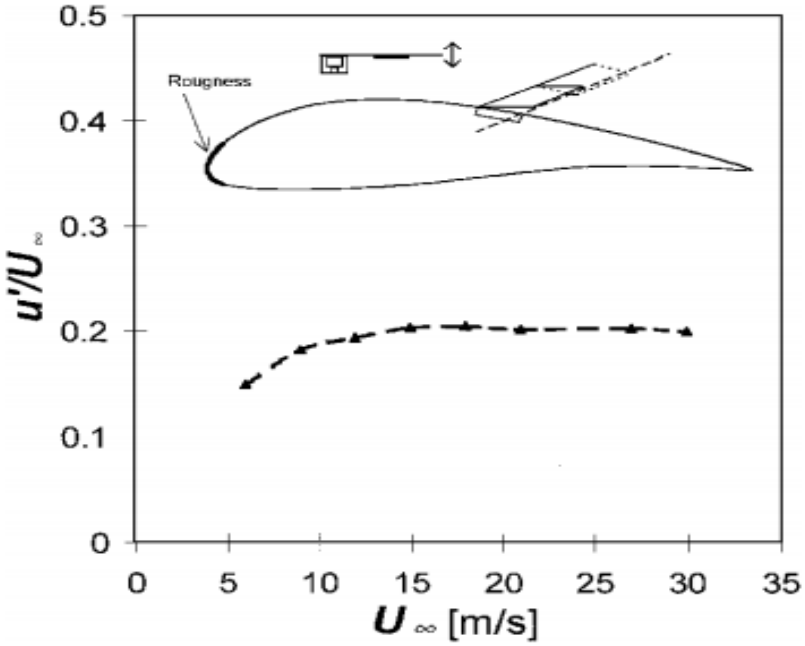

Outcomes:

The improvement in the aerofoil performance was measured at a single Reynolds number Rc=0.55X10^6 , using a tripped boundary layer and comparing the two modes of excitation—two dimensional and three dimensional—to the baseline.

Table 1 Summary of airfoil performance enhancement due to active separation control

		Mode		
Parameter	Explanation	Baseline	Two dimensional	Three dimensional
$C_{l_{max}}$	Maximum lift coefficient	1.26	1.51	1.54
α of $C_{l_{max}}$	Incidence at $C_{l,max}$	8	10	12
$C_{d,min}$	Minimum drag coefficient	0.0186	0.0145	0.0155
C_l of $C_{d,min}$		0.49	0.71	0.71
$L/D_{,max}$	Maximum lift/drag ratio	43	62	56.5
C_l of $L/D_{,max}$		0.9	1.3	1.1
L/D at $C_{l_{max}}/1.21$		43	61	53
η_{max}	Maximum power efficiency	43	38	48
C_l at η_{max}		0.89	1.40	1.09
$C_d + C_E$ at η_{max}	Total power coefficient	0.0206	0.0374	0.0228

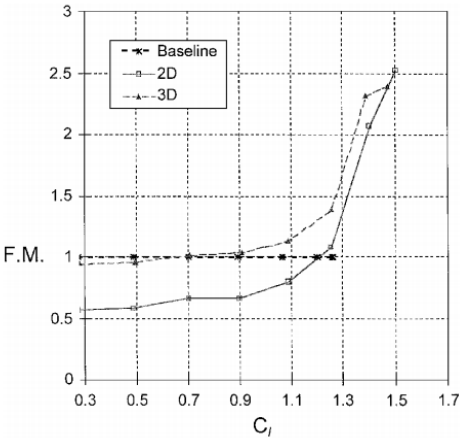

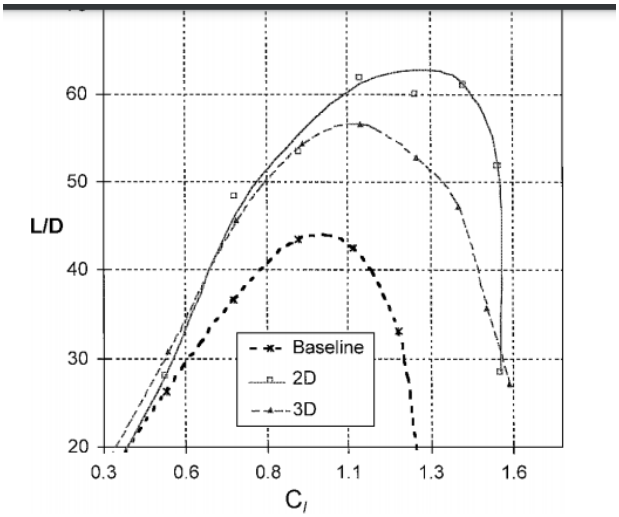

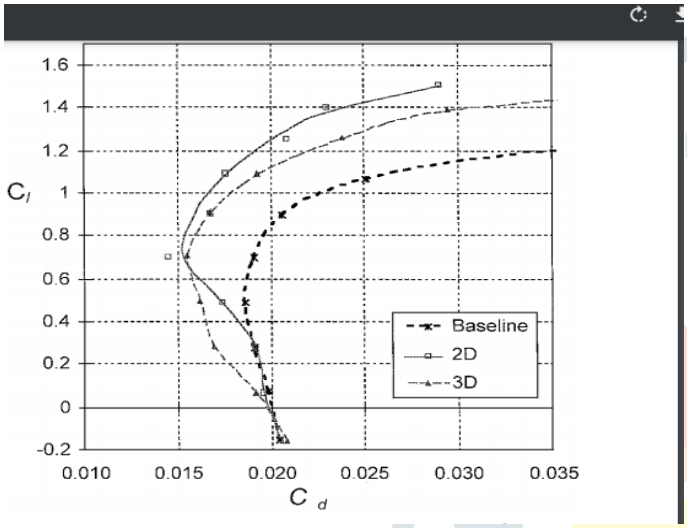

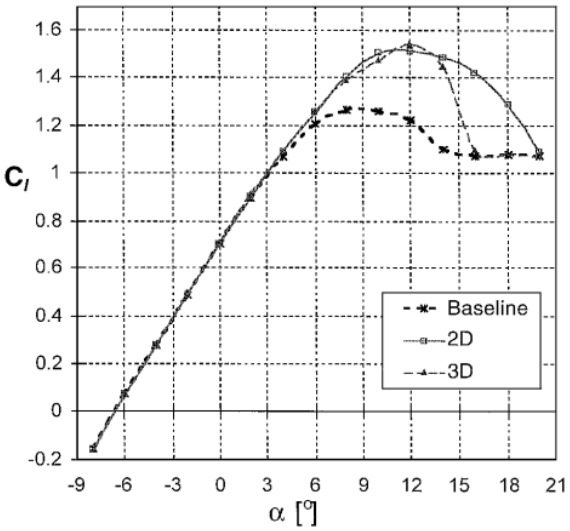

F.M=efficiency/(Cl/Cd)

Conclusion:

Observing the various aspects of the aerofoil performance,one can identify the following trends.

1) Clmax increases by 20–22%, regardless of the excitation mode. Considering the lower power consumption of the three-dimensional mode, it is certainly preferred for lift enhancement at landing configuration.

2) The two-dimensional mode generates the highest L/D at the highest Cl. The combination of high Cl at the highest L/D and mild post stall behavior makes the two-dimensional mode a suitable candidate for takeoff configuration.

The physical mechanism describing the nature of spanwise and streamwise vorticity generation by the two-dimensional and three dimensional modes and the interaction between the separating boundary layer and these disturbances was not studied. However, it is the first demonstration of energy-efficiency active flow-control.

LIFT ENHANCEMENT OF AN AEROFOIL USING A GURNEY FLAP AND VORTEX GENERATORS

Summary:

In this study attempts were made to enhance the lift by the introduction of Gurney flap and vortex generators on aerofoil . Gurney flap consist of small plate located at the trailing edge perpendicular to the pressure side of the aerofoil . Its height is 1-2% of the aerofoil chord. Analysis was done for the measurement of surface pressure distribution and wake profile for a NACA-4412 aerofoil to calculate the lift, drag and pitching-moment coefficient for different configurations of aerofoil with and without Gurney flap. Various studies were done for different Gurney flap height varying from 0.5%-3% aerofoil chord for the lift enhancement. Vortex generators were also used in this study. They generate the streamwise vortices, which energises the boundary layer and delay the flow separation which in turn increase the lift and aerofoil efficiency. The main objective of this study was to give an experimental data on the performance of Gurney flap on a single element aerofoil , different flap heights were analysed to determine the effect of Gurney flap height. The second objective of this was to determine the effectiveness of vortex generator in delaying the aerofoil stall.

Experimental Setup:

This experiment was conducted in 7ft-by-10ft closed-circuit wind tunnel at NASA Ames Research Centre. It is 15 ft long with 1% divergence with no turbulence reducing screen in the circuit and the turbulence intensity is 0.775 at 100 ft/s. A NACA-4412 aerofoil with chord 36 inch spanning the 10 ft width of wind tunnel was used. Boundary-layer trip strips were positioned at 2.5% and 10% chord on both upper and lower surface of wing. The aerofoil was mounted with 200 pressure taps on one spanwise and three chordwise rows. The lift and pitching-moment coefficient were determined by the centreline pressure taps, while two-dimensionality was measured by the rest of the pressure taps. The effect of Gurney flap size was determined first by using flap size varying from 0.5% to 2% chord. Wishbone vortex generators with height 0.5% chord were mounted across the span length at 12% chord from the leading edge.

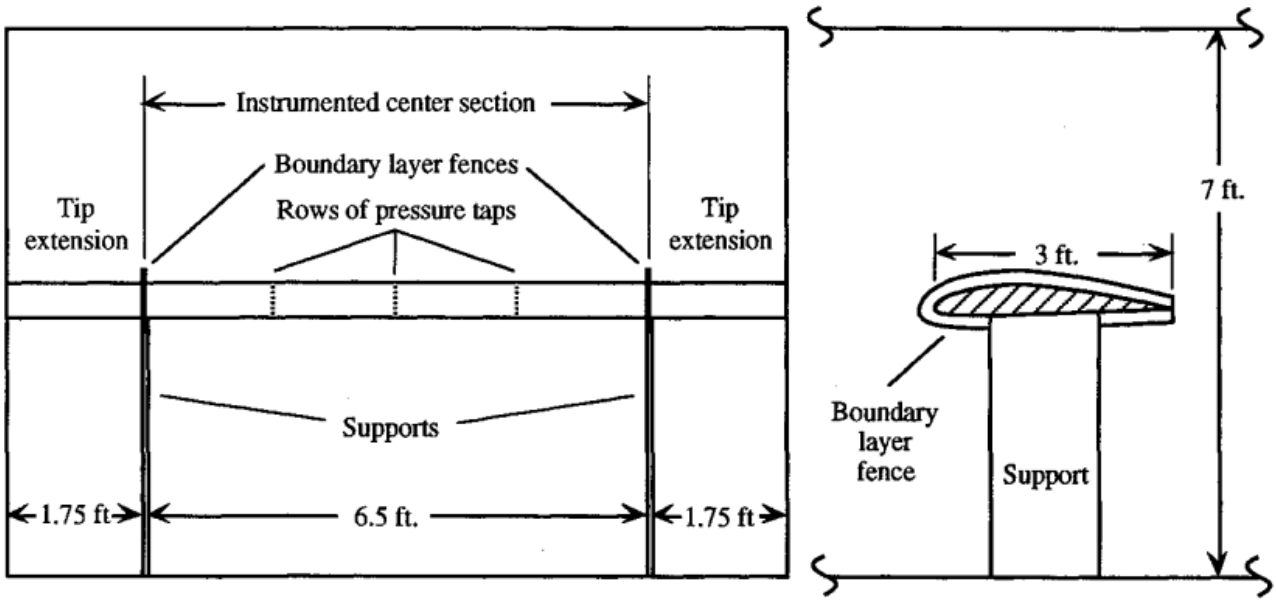

Fig. 3 NACA 4412 in the NASA Ames 7- by 10-ft Wind Tunnel test section.

Conclusion:

By the experimental data we gathered for the two lift-enhancing devices on a 2-D single-element aerofoil , we can conclude the following:

1. The Gurney flap can notably increase the maximum lift-coefficient and decrease the drag near maximum lift conditions, but an increase in drag was noticed at low to moderate lift coefficients.

2. Vortex Generators can certainly delay the flow separation and increase the maximum lift coefficient and they must be used in high lift systems.

3. The Gurney flap and vortex generators when used together can generate higher lift enhancements than either device individually.

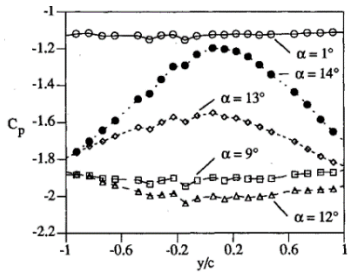

Fig. 4 Spanwise pressure coefficient variation at 0.25c for various angles of attack.

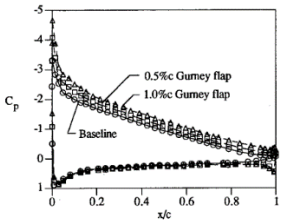

Fig. 6 Effect of Gurney flap height on chordwise pressure distribution at α = 9 deg.

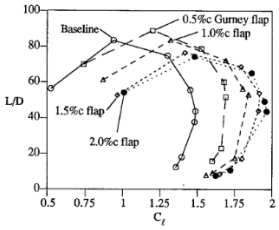

Fig. 8 Effect of Gurney flap height on lift-to-drag ratio.

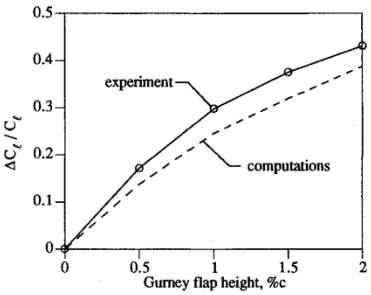

Fig. 15 Variation of lift coefficient increment with Gurney flap height.

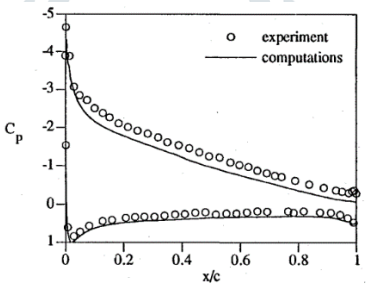

Fig. 13 Comparison of experimental and computed pressure distributions with a 1.0%c Gurney flap at α = 9 deg.

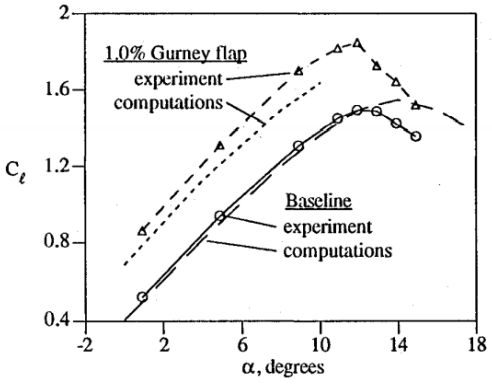

Fig. 14 Comparison of experimental and computed lift coefficient with and without a Gurney flap.

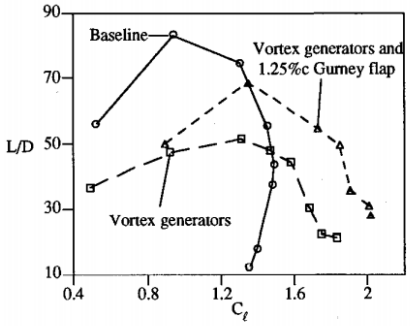

Fig. 17 Effect of vortex generators on the lift-to-drag ratio with and without a Gurney flap.

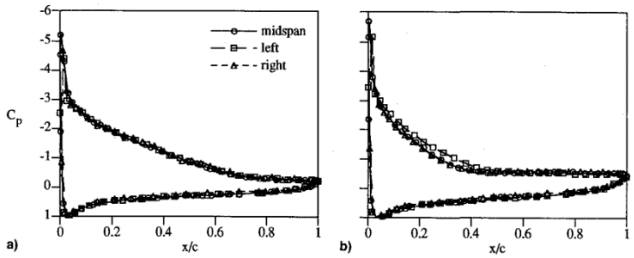

Fig. 5 Pressure distributions on the clean airfoil showing the character of the flow near and beyond $C_{l_{max}}$: a) α = 12 deg and b) α = 15 deg.

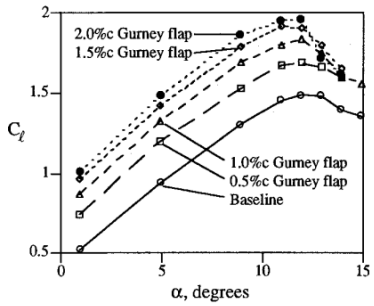

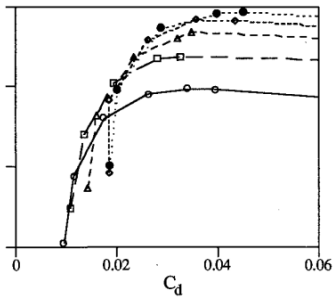

Fig. 7 Effect of Gurney flap height on the lift and drag coefficients.

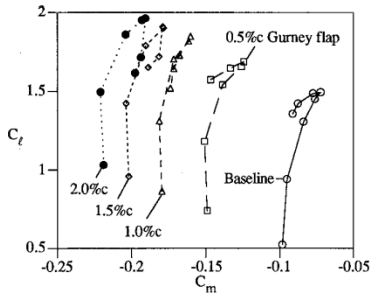

Fig. 9 Effect of Gurney flap height on pitching-moment coefficient.

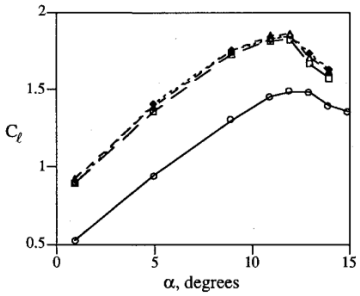

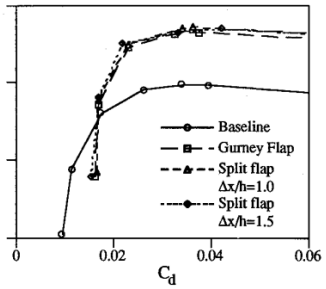

Fig. 11 Comparison of the Gurney flap and split flap configurations (h = 1.25%c).

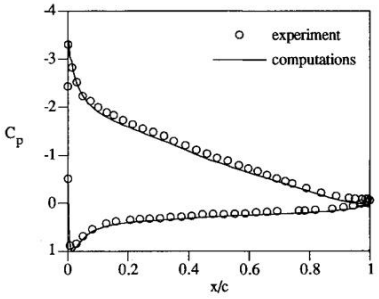

Fig. 12 Comparison of experimental and computed pressure distributions for the baseline airfoil at α = 9 deg.

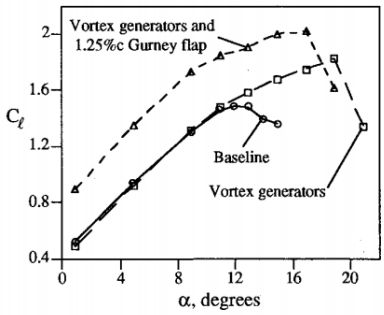

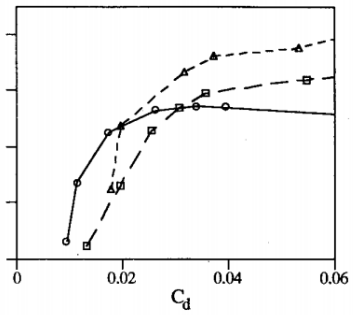

Fig. 16 Effect of vortex generators on the lift and drag coefficients with and without a Gurney flap.

Experimental Investigation of Jet Mixing of a Co-Flow Jet Aerofoil

Co-flow jet (CFJ) aerofoil jets are being investigated for the method of lifting the lift, the reduction of drag, and the increase of the folds in the stable.Digital Particle Image Velocimetry, visual acuity and aerodynamic power a scale used to demonstrate understanding of the CFJ aerofoil mixing process. At low AoA and low coefficient of pressure, the mixing between the wall plane and large flow is dominated by large corresponding structures of attached flow. As the tensile strength increases, the larger vortex structure disappears. At higher AoA with flow separation, CFJ creates a rising flow line in the middle both rotating shear calculator layer, i.e., external shear layer and internal flow caused by CFJ. The jet is cleaned in the usual way on the air surface defined by the seat point. With the greater the intensity of the CFJ pressure, the more the point remains down eventually disappears when the flow is attached. Chaos plays a major role in mixing

CFJ and main flow high throughput kinetic power from jet to main flow to keep the main flow attached at the top AoA produces high altitude. When the flow is divided, the increasing pressure of the CFJ. The coefficient also increases the turbulence in the jet injection mixing circuit.

Nomenclatures

AoA Angle of Attack C Chord length CC Circulation control CFD Computational Fluid Dynamics CFJ Co-Flow Jet CL Lift Coefficient CD Drag Coefficient Cμ Jet Momentum Coefficient D Drag L Lift LE Leading edge M Mach number p Static pressure Pt Total Pressure Re Reynolds number S Wing Span Area TE Trailing edge ZNMF Zero net mass flux m Jet mass flow rate u,v,w Velocity components in x-, y-, and z-direction V Velocity vector x,y,z chord, normal and spanwise directions, with respect to the aerofoil Subscripts: ∞ Freestream J Jet Greek Letters: γ Ratio of Specific Heats ρ Density α Angle of Attack β Angle between slot surface and the line normal to chord

All air flow and air-conditioning flexibility are available at the University of Miami 24 "x24" wind tunnel structures. Figure 2 and Fig. 3 showcases the overall look of the UM Aero-lab CFJ airlines and airports Conditions for flow and injection flow were present and it is governed independently. The compressor provides the injection flow line and flow rate is controlled using a computer-controlled KosoHammel Dahl computer valve. A Relax pump creates the minimum pressure required for pulling and is controlled with a hand needle valve. Both mass flow rates on injection and breastfeeding lines are measured using Orepac orifice mass flow meters fitted with high pressure MKS converts. Aerodynamics variables are measured using AMTI AM 6 elements transducers. All air tunnels in the freestream tunnel, CFJ air flow, and aerodynamic flexibility were present recorded using Labview's state-of-the-art data acquisition system. The LE trip has not been made since we found that the results do not matter the LE journey. All the details (e.g., wind tunnel speed, aerodynamics power, pulse and mass mobility) were obtained at an average rate of about 50 samples per second, which allows for limited air travel flutter analysis around stall angles. The range of attack angles (AoA) varies between 0o and 30o. The designated free streaming speed was V∞ = 10m / s for all tests and chords. Reynolds number was almost 1.89x10^5

With the growing AoA, the pressure on the aerofoil is expected to drop again facilitating entry of CFJ jets. This leads to a higher Cμ. Figure 4 shows the value of Cμ and jet velocity corresponding to all tests and shows that compensation was in place well achieved with low Cμ. In this paper, three values of Cμ at AoA = 0o introduced: 0.06, 0.15 and 0.25, corresponding to flow values of 0.030 kg / s, 0.045 kg / s and 0.060 kg / s, respectively. The speed of the jet varies accordingly about 23m / s, 34m / s, and 45m / s.

Various laser viewing techniques were used to monitor the broadcast above the upper area. LaVision Digital Particle Image Velocimetry (DPIV) Program with Litron Nano Nd: YAG 200 mJ / pulse used to monitor and detect speed field around the aerofoil . Pixel cross-correlation analysis 64x64 to 32x32. This method was used to cover the face with an air foot, which resulted in a total of 75x100 vectors (including aerofoil). A series of 1,000 velocity fields were obtained for each AoA at a time Cμ. Customized flow seeds using the same particles of PIV tracks used for flow visualization. Spark-guided movement was found to be within 1% root difference with tip, while sucking shows 7% doubt near the root aside. All presented results were received with category

B, in Fig. 3.

Results and Conclusion

Compared to the original base, the CFJ aerofoil shows great benefits to CL as well and is maintained at high Cμ values.

Great change in stability and drastic improvement in overall performance.

On low AoA and low coefficient of pressure, mixing between wall jet and mainflow is very high with large corresponding structures of the attached flow. When the intensity of the increase increases, the larger vortex structure disappears. At higher AoA with flow separation, CFJ creates a rising flow line in the middle both rotating shear calculator layer, i.e., external shear layer and internal flow caused by CFJ. UFS faces a large free vortex region. A joint wall the jet is cleaned in the usual way on the air surface defined by the seat point. With the greater the intensity of the CFJ pressure, the more the point remains down eventually disappears when the flow is attached. Chaos plays a major role in mixing CFJ and mainflow high throughput kinetic power from jet to mainflow to keep the mainflow attached at the top AoA produces high altitude. When the flow is divided, the increasing pressure of the CFJ. The coefficient also increases the turbulence in the jet injection mixing circuit. What flow is attached, the kinetic kinetic energy is greatly reduced due to the disappearance of vortices of the main building.

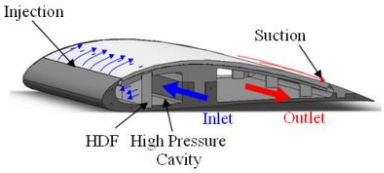

Fig. 1. Schematic and concept of CFJ airfoil

Fig. 2 Wind tunnel facility

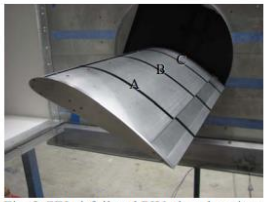

Fig. 3 CFJ airfoil and PIV plans locations

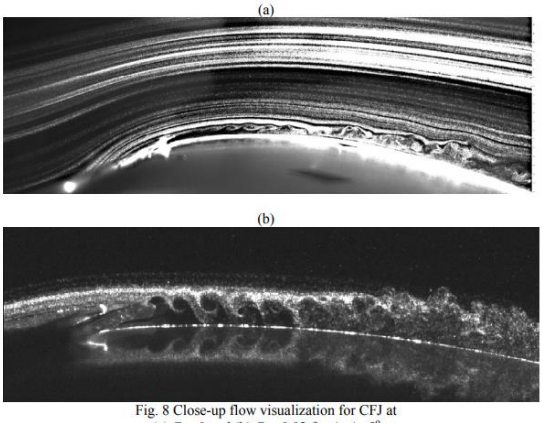

Fig. 8 Close-up flow visualization for CFJ at (a) Cμ=0 and (b) Cμ=0.02 for AoA=5°

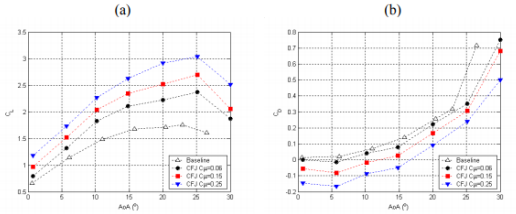

Fig. 5 Lift and Drag coefficient results comparison for baseline and CFJ at various AoA and Cμ

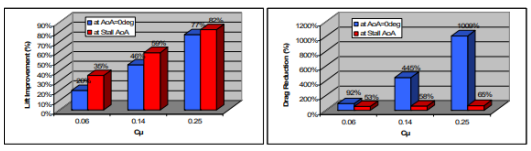

Fig. 6 Performance enhancement at zero AoA and stall AoA.

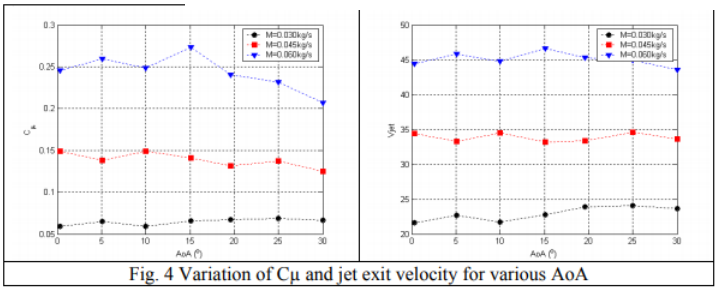

Fig. 4 Variation of Cμ and jet exit velocity for various AoA

REFERENCE

[1] J V MurugalalJeyan, Bilji C Mathew, Vijay Kumar Singh "Flow Separation Analysis For Various Angle of Attack on NACA 4412 Aerofoil A Computational Approach "THINK INDIA JOURNAL ISSN: 0971-1260. Vol. 22, Issue 17, September-2019 page no 1352

[2] JV MurugaLalJeyan, Kavya S nair, SagarikaMaiti "Computational And Experimental Study On Variable Area Ducts For Various FlowConditions - A Comparative study" journal of the Gujarat research society ISSN: 0374-8588Volume 21 Issue 8s, November 2019 page 91-99

[3] J.V. MurugaLalJeyan, Krishna S Nair*, Godwin Vincent"CFD Analysis on Various Commercial Vehicles to Evaluate the Aerodynamic Characteristics - A Comparative Study "Journal of Advanced Engineering Research December 2019, Volume 6, Issue 2 page 59-63

[4] J V MurugalalJeyan ,Dr. M. Senthil Kumar , "Performance Evaluation for Multi-Hole Probe With the Aid of Artificial Neural Network" International Journal of Theoretical and Applied Information Technology (JTAIT). ISSN 1992-8645Vol No: 65 , Issue 3 , PP: 665 July 31, 2014

[5] J V MurugalalJeyan , Dr. M. Senthil Kumar, "Performance Evaluation of Yaw Meter With the Aid of Computational Fluid Dynamic" , International Review of Mechanical Engineering (IREME). ISSN: 1970-8734, Vol No. 8,Issue 02

[6] J V MurugalalJeyan,Krishna S nair , Kavya S nair "The Low Speed Aerodynamic Analysis Of Segmental Wing Profile "International Journal of Mechanical and Production Engineering Research and Development (IJMPERD) ISSN (P): 2249–6890; ISSN (E): 2249–8001 Vol. 9, Issue 4, Aug 2019, 1303–1310

[7] J V MurugalalJeyan, Shreyashkailashoval, Tenzintadin&Harmeet Singh "Aerodynamic Design And Computational Analysis Of Vented Naca2412 Airfoil- A Comparative Study "International Journal of Mechanical and Production Engineering Research and Development. Vol. 10, Issue 1, Jan 2020, 283–294

[8] JV MurugaLalJeyan, Kavya S Nair and Krishna S Nair "Aerodynamics and flow pattern performance evaluation of offroad vehicle for various velocity range and angle of incidence" Journal of Physics: Conference Series, volume/ issue 1473 march 2020 012001

[9] R. SabariVihar, J. V. MurugaLalJeyan, K. SaiPriyanka. (2020). A Review on Aerodynamic Parameters, Methodologies and Suppression Techniques Explored in Aircraft Wing Flutter. International Journal of Advanced Science and Technology

[10] K.SaiPriyanka , J V MurugaLalJeyan*, R.SabariVihar. (2020). A Review on a Reassess Swot up on Airfoil Stall and Flow Separation Delay for a Range of Limitations Associated with Aerodynamics and Wing Profile. International Journal of Advanced Science and Technology, 29(06), 7659-7668

[11] Ramesh PS, JV Muruga lal jeyan Mini Unmanned Aerial Systems (UAV) - A Review of theParameters for Classification of a Mini UAV - International Journal of Aviation,Aeronautics, and Aerospace , Published by Scholarly CommonsEmbry-Riddle Aeronautical University Volume 7 Issue 3 Article 5 2020

[12] Ramesh, P.S. and MurugaLalJeyan, J.V. (2021), "Terrain imperatives for Mini unmanned aircraft systems applications", International Journal of Intelligent Unmanned Systems, Vol. ahead-of-print No. ahead-of-print. https://doi.org/10.1108/IJIUS-09-2020-0044

[13] Balaji R, J V MurugaLalJeyan, Vijay Kumar singh "Review on influence of radiating and aerodynamic shock athypersonic vehicle" Journal of Physics: Conference Series, volume/ issue 1473 march 2020 012004